Influence of manganese on the phase composition and mechanical properties of Al-Zn-Mg-Cu-Zr-Y(Er) alloys

M. V. Glavatskikh · R. Yu. Barkov · M. G. Khomutov · A. V. Pozdniakov

Received: 3 May 2023 / Revised: 23 May 2023 / Accepted: 15 October 2023 / Published online: 14 May 2024

Abstract
The effect of alloying with manganese and titanium on phase composition and mechanical properties of new Al-Zn-Mg-Cu-Zr-Y(Er) alloys is studied using thermodynamic calculations, scanning electron microscopy, and X-ray phase analysis. Introduction of manganese into AlZnMgCuZrY and AlZnMgCuZrEr alloys leads to formation of $(Al,Cu)_{11}Y_3$, $Al_{25}Cu_4Mn_2Y$, and $Al_{25}Cu_4Mn_2Er$ phases respectively, in which up to 12 wt.% Zn is dissolved, which replaces aluminum atoms within the phase lattice. In the process of homogenization for phases enriched in yttrium or erbium hardly change their morphology, while T(Al,Zn,Mg,Cu) phase dissolves and transforms into the S(Al_2CuMg) phase. In this case, according to calculations, Al_6Mn, Al_3Zr, and Al_3Ti phases are present in equilibrium with (Al). Microstructural studies confirm presence of particles within aluminum solid solution (Al), i.e. heterogenization proceeds in parallel with homogenization. The course of heterogenization provides 7–15 HV greater hardness for alloys with manganese in a quenched condition, but they have a less alloyed solid solution in terms of Zn, Mg, and Cu, which reduces hardening during aging. Alloys doped with manganese and titanium are hardly inferior in terms of yield strength, and when temperature rises to 300–350 °C, they slightly surpass alloys without them. Modification with titanium leads to grain refinement, which contributes to yield strength, partly compensating for the lower alloying (Al).

Keywords Aluminum alloys · Erbium · Yttrium · Microstructure · Phase composition · Aging · Compression

Alloys of the Al-Zn-Mg-Cu system concern a group of high-strength wrought alloys. In view of features of the composition (Zn/Mg>1) these alloys have high corrosion resistance and heat resistance, high strength at room temperature, although the technological efficiency during casting, corrosion resistance, and heat resistance are low [1–4]. With a reduction in zinc content and adjustment of the Zn/Mg ratio alloys start to be inferior with respect to strength but there is an improvement in their corrosion resistance, thermal stability, and casting properties are improved [1, 2, 4–6]. In addition an increase in technological efficiency during casting, and strength and heat resistance is possible by alloying with eutectic-forming elements [5–11]. Alloying with rare-earth metals, and in particular zirconium [10–20], or zirconium with other rare-earth elements and transition metals [18–33] leads to formation of nanosize strengthening dispersoids. Also zirconium as a grain modifier facilitates an improvement in technological efficiency during casting [4]. Under these alloying conditions and associated heat treatment a structure is formed within alloys with compact particles of crystallization origin and nanosize dispersoids that make it possible to achieve a good combination of properties [34–39]. Also, alloying with yttrium or erbium [40–49] has a complex effect on the phase composition and microstructure, which

Translated from *Metallurg*, No. 12, pp. 47–53, December, 2023.

during crystallization pass into the composition of aluminum solid solution and form a fine eutectic. During subsequent annealing yttrium and erbium pass into the composition of dispersoids, increasing the density of their precipitation and eutectic phase particles are fragmented, spheroidized and demonstrate high coagulation resistance [43–49]. In [50] the effect on phase composition and properties of alloying Al-Zn-Mg-Cu-Zr with an increased copper content with yttrium or erbium is studied. It is shown that alloys with yttrium or erbium are distinguished by better technological efficiency and failure resistance with overageing. An additional increase in aluminum alloy strength properties at room and elevated temperatures may be achieved by alloying with manganese up to 1%, which leads to formation during homogenization of $Al_{20}Cu_3Mn_3$ phase dispersoids [51]. *The aim of this work* is determination of the effect of manganese on the phase composition and metal properties of Al-Zn-Mg-Cu-Zr-Y(Er) alloys additionally modified with titanium.

Research materials and methods. Alloys of Al (99.99%), Zn (99.9%), Mg (99.9%), Cu (99.9%), master alloys Al-5Zr, Al-5Ti-1B, Al-10Mn, Al-10Y and Al-9Er were prepared in a resistance furnace. Casting at 800 °C was performed into a graphite mold with a cooling rate of about 15 °C/s. The size of an ingot obtained was 15 x 60 x 150 mm. According to results of determining the composition by micro X-ray spectrographic analysis in a scanning electron microscope (SEM) alloys contained (wt. %): 4.5-4.7 Zn, 3.4-3.5 Mg, 2.5 Cu, 0.7-0.8 Mn, 0.2 Zr, 0.1 Ti (alloy AlZnMgCuMnTi) and 0.4 Y (alloy AlZnMgCuMnTiY) or 1 Er (alloy AlZnMgCuMnTiEr), balance aluminum. The confidence range in determining the zinc, magnesium, and copper content within alloy and aluminum slid solution did not exceed 0.2%. Calorimetric analysis was conducted in a differential scanning calorimeter (DSC). According to DSC analysis the alloy solidus temperature was 477 °C. Heat treatment was carried out in a Nabatherm and Snol furnaces with a fan, and temperature maintenance precision of 1 °C. Ingot homogenization was carried out at 465 °C for 1, 3, and 6 h. After 3 h of homogenization at 465 °C alloy specimens were quenched and aged at 120, 150, 180, 210 and 250 °C for a different time. Sections were prepared for microstructural studies that was accomplished in Struers Labopol-5 digital-polishing unit. Microstructural studies and identification of phases was carried in a Neophot light microscope (LM) and a TESCAN VEGA 3LMH (SEM) with an energy dispersion electrode X-Max 80 Labsys Setaram. Alloy specimen grain structure was studied in polarized light in the SEM. Oxidation (15–25 V, 0–5 °C) was conducted in Barker solution (46 ml HBF_4, 7 g HBO_3 and 970 ml H_2O) using a lead cathode. X-ray phase analysis was carried out in a Brucker D8 Advanced diffractometer with CuK_α radiation. Thermodynamic calculations were carried out using a Thermoclac program in in a TCAL4 database. Hardness was measured by a standard Vickers method. A Gleeble-3800 complex was used for testing in compression at a rate f 4 mm/min at room and elevated temperature of 200–350 °C.

Results and discussion

A test alloy ingot microstructure is presented in Fig. 1. In alloy AlZnMgCuMnTi on a background of aluminum solid solution (Al) a fine eutectic, intermetallic phases that contain Zn, Mg and Cu are present according to element distribution maps between phases. Intermetallic particles correspond to the phase T(Al,Zn,Mg,Cu). A similar structure is formed in an alloy ingot without magnesium and titanium [33]. Mn, Zr, and Ti are uniformly distributed within matrix (Al) (see Fig. 1a). Within alloy with yttrium AlZnMgCuMnTiY apart from phase T, three different phases crystallize (see Fig. 1b). White particles are enriched with Cu and Y, and point analysis in an SEM shows presence within these particles of just 8–10% Zn, 2–3% Mg and 1% Mn (here and subsequently through the text of the article wt.% is used). With respect to composition particles are similar to Al_8Cu_4Y phase, although their main peaks at angles 40–42° within an X-ray diffraction pattern are not revealed (Fig. 2b). Peaks at angles 36–37.5° in an X-ray diffraction pattern probably correspond to $(Al,Cu)_{11}Y_3$, phase, whose presence is noted in ternary alloy Al-Cu-Y [40]. In this case zinc atoms may displace Al within the phase lattice and magnesium and manganese are captured during analysis of (Al). Then the formula of the phase may

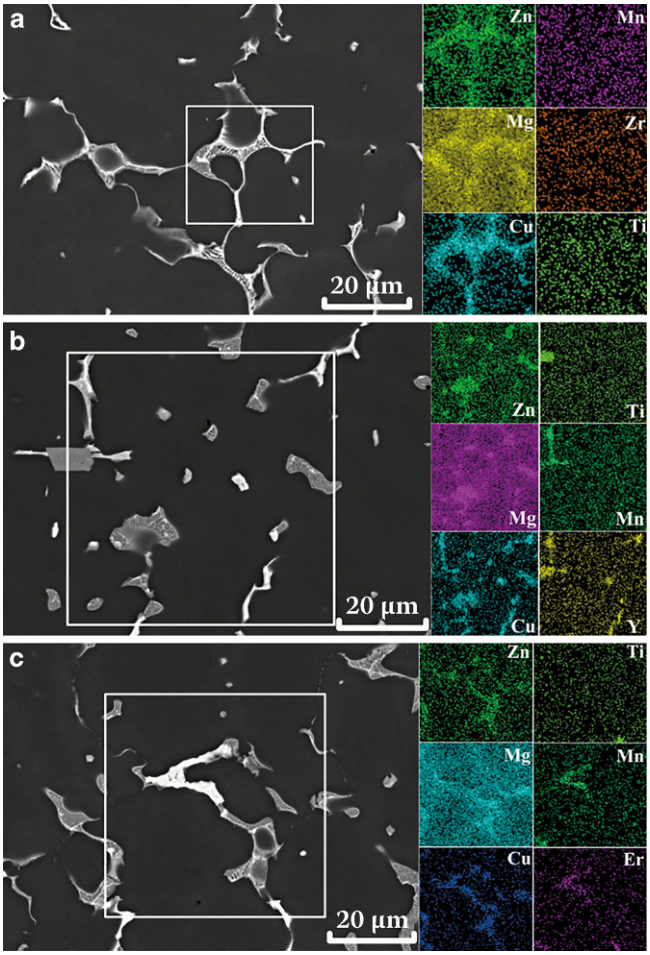

Fig. 1 Microstructure of ingots of alloys AlZnMgCuMnTi (**a**), AlZnMgCuMnTiY (**b**) and AlZnMgCuMnTiEr (**c**) and alloying element distribution between phases within separated region (SEM)

be written as $(Al,Cu,Zn)_{11}Y_3$. A second type of particles (enriched with Cu (20–25%), Y (8–10%) and Mn (12–14%)), within which about 12% Zn is also noted, probably corresponds to a fourth phase $Al_{25}Cu_4Mn_2Y$ [46], within which Zn replaces part of the Al. In addition within the structure a small amount is revealed of undesirable primary crystals containing Ti and Y within the composition, which correspond to $Al_3(Ti,Y)$ phase. Within AlZnMgCuMnTiEr alloy apart from (A)l and Ti there is presence of particles of a phase rich in Cu (20–25%), Er (16–20%) and Mn (10–12%) and containing ≈10% Zn (Fig. 1c). These particles correspond to the phase $Al_{25}Cu_4Mn_2Er$, determined within alloy Al-Cu-Er-Mn-Zr [45], within which Zr atoms also replace Al. According to element distribution maps and point analysis within the structure there is also presence of primary crystals of $Al_3(Ti,Er)$ phase (Fig. 1c), and X-ray phase analysis demonstrates presence of peaks from phases Al_8Cu_4Er and Al_3Er (Fig. 2c). In a cast condition the average content of the main dissolved strengtheners Zn (2.7–3%), Mg (1.8–2.3%) and Cu (0.6%) is somewhat lower than in alloys without manganese (Table 1).

Alloying with manganese does not affect the alloy solidus temperature. Evolution of the microstructure and phase composition of alloys during homogenization before quenching is presented in Figs. 3, 4 and 5. Within alloy AlZnMgCuMnTi due to dissolution of a non-equilibrium excess phase of crystallization origin the concentration of Zn, Mg, and Cu within (Al) increases to 4.7–5.0, 3.5 and 1.1–1.4% respectively. Phase T in this case is replaced entirely by phase S (Al_2CuMg), which is in good agreement with results of thermodynamic calculations. In this case in equilibrium with (Al), according to thermodynamic calculation, at 465 °C there also presence of Al_6Mn, Al_3Zr and Al_3Ti phases which should separate from (Al) solution during crystallization

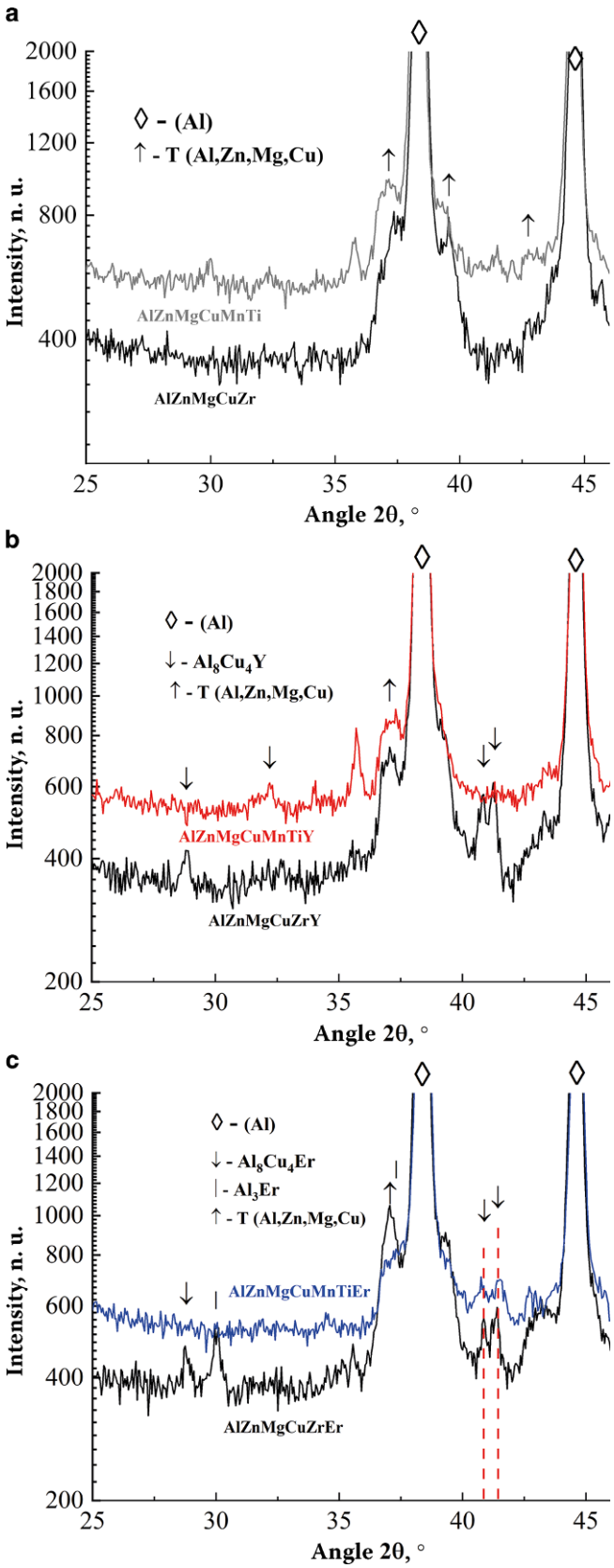

Fig. 2 X-ray diffraction patterns for ingots of alloys AlZnMgCuMnTi (**a**), AlZnMgCuMnTiY (**b**) and AlZnMgCuMnTiEr (**c**) compared with alloys without manganese and titanium

 https://doi.org/10.1007/s11015-024-01683-9

Table 1 Composition (Al) in wt.% in Cast Condition and After Quenching from 465 °C with Preliminary Homogenization for 1, 3, and 6 h

Alloy	Cast condition			1 h			3 h			6 h		
	Zn	Mg	Cu	Zn	Mg	Cu	Zn	Mg	Cu	Zn	Mg	Cu
AlZnMgCuZr	3	2.5	0.6	5	4	1	5	4	1.1	5	4	1.1
AlZnMgCuMnTi	2.7	2	0.6	4.7	3.5	1.1	4.9	3.5	1.3	5	3.5	1.4
AlZnMgCuZrY	3	2.6	0.7	4.9	4.2	1	5	4.4	1	5	4.4	1.1
AlZnMgCuMnTiY	3	2.3	0.6	4	3.2	1.1	4.5	3.5	1.2	4.6	3.6	1.4
AlZnMgCuZrEr	3	2.5	0.7	4.5	4.2	1	4.8	4.3	1	4.9	4.3	1
AlZnMgCuMnTiEr	2.7	1.8	0.6	4.4	3.2	1	4.5	3.5	1.2	4.7	3.5	1.2

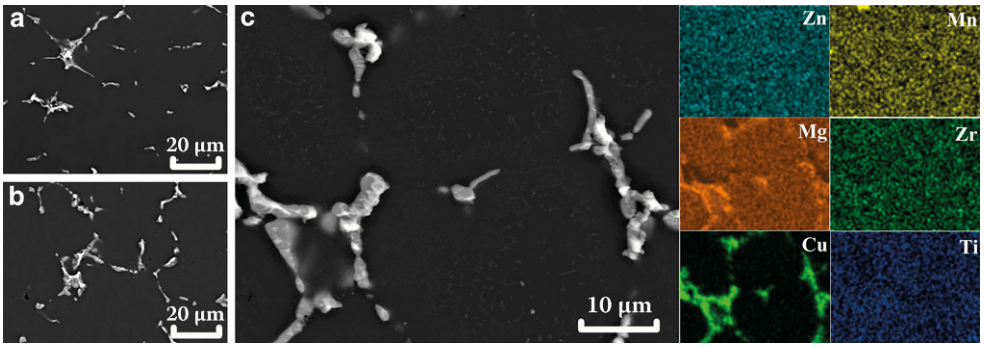

Fig. 3 Microstructure of alloy AlZnMgCuMnTi after quenching from 465 °C with preliminary homogenization for 1 (**a**), 3 (**b**), and 6 (**c**) h and alloying element between phases after 6 h (SEM).distribution

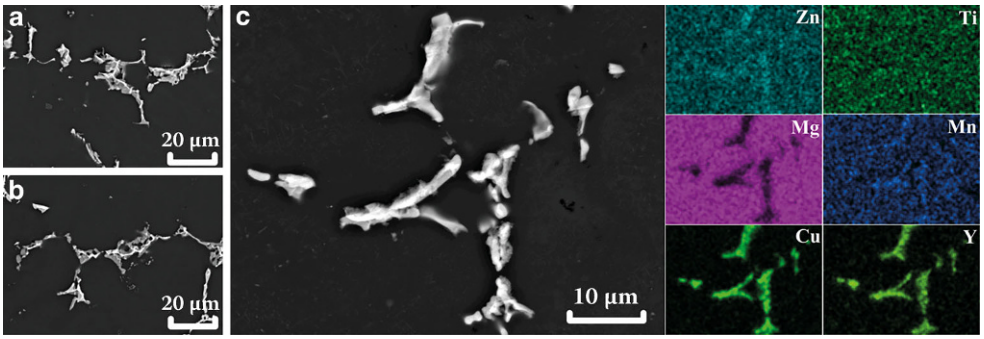

Fig. 4 Microstructure of alloy AlZnMgCuMnTiY after quenching from 465 °C with preliminary homogenization for 1 (**a**), 3 (**b**), and 6 (**c**) h and alloying element between phases after 6 h (SEM).distribution

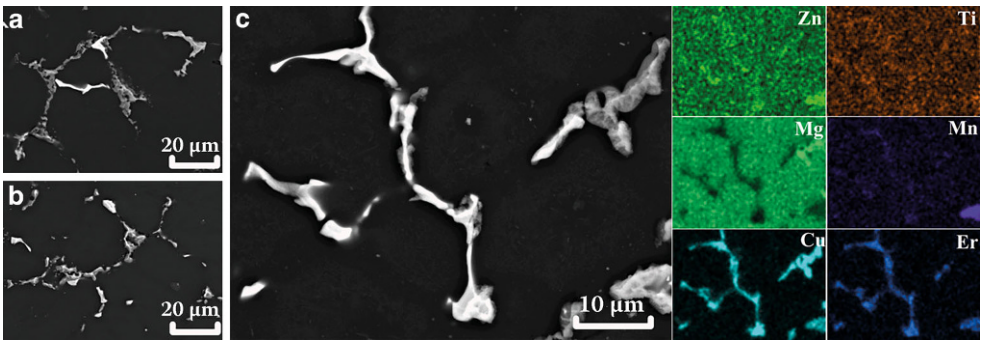

Fig. 5 Microstructure of alloy AlZnMgCuMnTiEr after quenching from 465 °C with preliminary homogenization for 1 (**a**), 3 (**b**), and 6 (**c**) h and alloying element between phases after 6 h (SEM).distribution

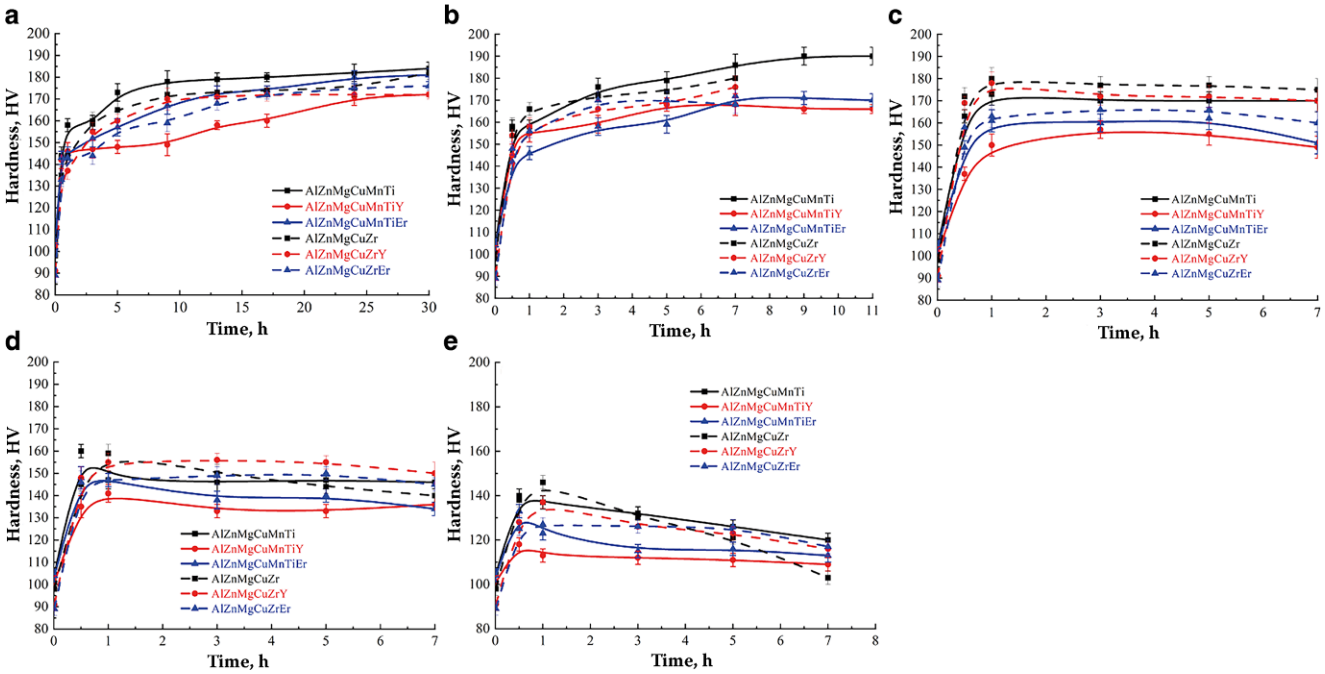

Fig. 6 Dependence of hardness HV on aging time after quenching from 465 °C with previous homogenization for 3 h (broken line for alloys without manganese and titanium). (**a** 120 °C, **b** 150 °C, **c** 180 °C, **d** 210 °C and **e** 250 °C)

supersaturated with respect to Mn, Zr, and Ti. In an SEM image (see Fig. 3) a greater amount of light dispersed inclusions is seen within the matrix (Al), i.e., in parallel with homogenization there is heterogenization.

During homogenization annealing of alloys AlZnMgCuMnTiY and AlZnMgCuMnTiEr there are the same processes. The content of Zn, Mg and Cu within (Al) increases to 4.5–4.7; 3.5–3.6 and 1.2–1.4% respectively (see Table 1), and as a result there is dissolution of T-phase and transformation into phase S. In solid solution a considerable amount of fine particles is present of a phase formed as a result of breakdown of (Al). The main difference is presence within solution of ~0.2% Y and Er, which should dissolve in Al_3Zr particles increasing the density if their separation [42–46].

Formation after quenching from 465 °C with preliminary homogenization for 3 h of a difference in microstructure and composition (Al) in alloys with and without manganese (See Table 1) points to a visible effect on alloy ageing kinetics. Manganese within alloys based upon Al may lead to formation of dispersoids of $Al_{20}Cu_2Mn_3$ [45, 46]. In addition in within alloys with manganese at 0.5% lower than the magnesium content, which reduces the volume fraction of ageing products and may change their type. Dependences are provided in Fig. 6 for hardness on ageing time at temperatures 120, 150, 180, 210 and 250 °C compared with alloys without manganese and titanium [50]. Alloys without manganese and titanium AlZnMgCuZr, AlZnMgCuZrY and AlZnMgCuZrEr in a quenched condition have a hardness of 98 HV, 91 HV and 89 HV [33], and within alloys studied with manganese and titanium it is 105 HV, 101 HV and 104 HV respectively. The greater hardness is provided separation of dispersoids of supersaturated material during crystallization (Al), i.e., heterogenization during homogenization annealing before quenching. In this case due to the lower alloying capacity of (Al) in test alloys a lower strengthening effect is achieved due to ageing (see Fig. 6). For comparison in Fig. 6 shown by broken lines is the dependence of hardness on ageing time for alloys AlZnMgCuZr, AlZnMgCuZrY and AlZnMgCuZrEr [50]. An increase in hardness in the test alloys by 10–20 HV is lower than in alloys without manganese and titanium, but ageing kinetics are not markedly different.

Values are provided in Table 2 for yield strength in compression at different temperatures after quenching from 465 °C with preliminary homogenization for 3 h and ageing at 180 °C for 3 h. Alloying with manganese and titanium for the alloy hardly changes with respect to the level of yield strength, and at room temperature

Table 2 Yield Strength in Compression (MPa) at Different Temperatures after Quenching and Aging at 180 °C for 3 h

Alloy	20 °C	200 °C	250 °C	300 °C	350 °C
AlZnMgCuZr	435 ± 10	360 ± 5	295 ± 5	175 ± 10	92 ± 5
AlZnMgCuMnTi	470 ± 10	322 ± 5	290 ± 15	177 ± 5	105 ± 10
AlZnMgCuZrY	420 ± 15	335 ± 15	265 ± 5	167 ± 5	95 ± 5
AlZnMgCuMnTiY	467 ± 15	320 ± 10	263 ± 5	178 ± 5	91 ± 5
AlZnMgCuZrEr	460 ± 15	335 ± 15	285 ± 5	162 ± 5	89 ± 5
AlZnMgCuMnTiEr	462 ± 20	305 ± 5	237 ± 10	180 ± 5	101 ± 5

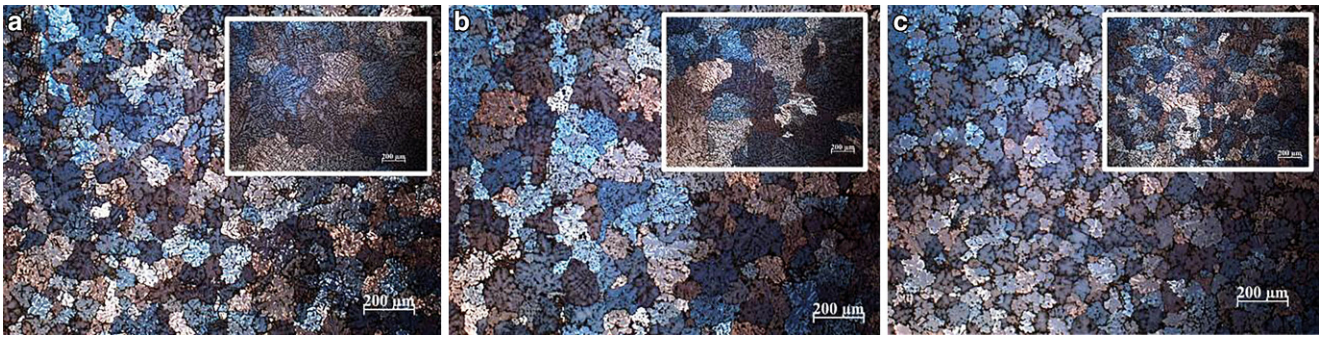

Fig. 7 Ingot microstructure for alloys AlZnMgCuMnTi (**a**), AlZnMgCuMnTiY (**b**) and AlZnMgCuMnTiEr (**c**) (inserts are alloys without titanium and manganese at the same magnification) (SM)

up to 300–350 °C a trend is even observed towards prevalence over yield strength for alloys without Mn and Ti. In this case alloys modified with titanium has less effect on grain size (Fig. 7), which makes a noticeable contribution to the values of yield strength, compensating lower alloying of (Al). Alloys modified with titanium with titanium AlZnMgCuMnTi, AlZnMgCuMnTiY, AlZnMgCuMnTiEr have a grain size of 62 ± 4, 87 ± 7 and 57 ± 3 μm, whereas for alloys without it the grain size is 166 ± 25, 173 ± 23 and 87 ± 7 μm respectively (see Fig. 7). It is noted that the alloys studied in this work have greater yield strength values in compression at elevated temperature than for example new heat-resistant alloys based upon the system Al-Cu-Y(Er)-Mn-Zr-Ti-Mg [48], and many industrial alloys of the system Al-Zn-Mg-Cu at 250 °C [51, 52]. This situation is the main achievement of the new alloys.

Conclusions

1. Addition of manganese into alloy AlZnMgCuZrY leads to formation of $(Al,Cu)_{11}Y_3$ and $Al_{25}Cu_4Mn_2Y$ phases, and within AlZnMgCuZrEr alloy there is crystallization of $Al_{25}Cu_4Mn_2Er$ phase. In this case within these phases up to 12% Zn dissolves, which replaces aluminum atoms within the lattice of phases.
2. During homogenization phases enriched in yttrium or erbium hardly change their morphology, but phase T dissolves and is transformed into S phase. In this case in equilibrium with (Al) according to thermodynamic calculations there is presence of phases Al_6Mn, Al_3Zr and Al_3Ti. Microstructural studies confirm presence of particles within (Al), i.e., in parallel with homogenization there is heterogenization.
3. Heterogenization provides hardness greater by 7–15 HV for alloys with manganese in a quenched condition, but they have a less alloyed solid solution with respect Zn, Mg, and Cu content, which reduces strength during ageing.

4. Alloys containing manganese and titanium are hardly surpassed with respect to the level yield strength, and with an increase in temperature to 300–350 °C they somewhat surpass alloys without manganese and titanium. Modification with titanium leads to grain refinement, which contributes to the yield strength value, partly compensating lower alloy content (Al).

Funding This study was supported by the Russian Science Foundation grant No. 22–79–10142, https://rscf.ru/project/22-79-10142/.

References

1. Gerchikova NS, Fridlyander IN, Zaitseva NI, Kirkina NN (1972) Change in the structure and properties of Al-Zn-Mg alloys. Met Sci Heat Treat 14(3):233–236
2. Zolotorevskii VS (1978) Aluminum Alloy Microstructure and Mechanical Properties. MISiS, Moscow (Diss. Doc. Techn. Sci)
3. Zou Y, Wu X, Tang S, Zhu Q, Song H, Guo M, Cao I (2021) Investigation on microstructure and mechanical properties of Al-Zn-Mg-Cu alloys with various Zn/Mg ratios. J Mater Sci Tech 85:106–117
4. Novikov II (1966) Nonferrous metal and alloy heat capacity. Nauka, Moscow (in Russian)
5. Cheverikin VV (2007) Effect of element eutectic formation on properties of high-strength alloys of the Al-Zn-Mg system. MISiS, Moscow (Diss. Cand. Techn. Sci)
6. Pan Y, Zhang D, Liu H, Zhuang L, Zhang J (2021) Precipitation hardening and intergranular corrosion behavior of novel Al-Mg-Zn(-Cu) alloys. J All Comp 853:157199
7. Zolotorevskiy VS, Pozdniakov AV, Yu A (2014) Churyumov, "Search for promising compositions for developing new multiphase casting alloys based on Al-Zn-Mg matrix using thermodynamic calculations and mathematic modelling,". Phys Met Metallogr 115(3):286–294
8. Pozdniakov AV, Zolotorevskiy VS, Mamzurina OI (2015) Determining the hot cracking index of Al-Mg-Zn casting alloys calculated using the effective solidification range. Int J Cast Met Res 28(5):318–321
9. Shurkin PK, Akopyan TK, Galkin SP, Aleshchenko AS Effect of radial shear rolling on the structure and mechanical properties of a new-generation high-strength aluminum alloy based on the Al-Zn-Mg-Ni-Fe system. Met Sci Heat Treat 60:764–769
10. Belov NA, Zolotozarevskii VS (2003) Cast alloys based upon aluminum-nickel eutectic (nickalins) as a possible alternative to silumin. Tsvet Met (2):99–105
11. Belov NA, Zolotozarevskii VS (2003) New high strength cast alloys based upon aluminum-nickel eutectic (nikalins). Scientific and technological provision of activity of enterprises, institutes and firms: Mater. Seminar. MGIU, Moscow
12. Ryum N (1969) Precipitation and recrystallization in an Al-0.5 wt.% Zr-alloy. Acta Met 17:269–278
13. Nes E, Billdal H (1977) The mechanism of discontinuous precipitation of the metastable Al_3Zr phase from an Al-Zr solid solution. Acta Met 25:1039–1046
14. Knipling KE, Dunand DC, Seidman DN (2007) Nucleation and precipitation strengthening in dilute Al-Ti and Al-Zr alloys. Met Mater Trans A 38:2552–2563
15. Belov NA, Alabin AN, Yu. Prokhorov A (2009) Effect of adding zirconium on strength and electrical resistance of cold-rolled aluminum sheets. Izv Vuzov Tsvet Met (4):42–47
16. Belov NA, Alabin AN, Yu. Prokhorov A (2009) Effect of annealing on electrical resistance and mechanical properties of cold deformed alloy Al-0.6% (wt.) Zr. Tsvet Met (10):65–68
17. Souza PHL, de Oliveira CAS, do Vale Quaresma JM (2018) Precipitation hardening in dilute Al-Zr alloys. J Mater Res Tech 7:66–72
18. Zakharov VV, Fisenko IA (2018) Effect of homogenization on the structure and properties of alloy of the Al-Zn-Mg-Sc-Zr system. Met Sci Heat Treat 60:354–359
19. Knipling KE, Dunand DC, Seidman DN (2008) Precipitation evolution in Al-Zr and Al-Zr-Ti alloys during isothermal aging at 375–425 °C. Acta Mater 56:114–127
20. Knipling K (2008) Precipitation evolution in Al-Zr and Al-Zr-Ti alloys during aging at 450–600 °C. Acta Mater 56:1182–1195
21. Fuller CB, Seidman DN, Dunand DC (2003) Mechanical properties of Al(Sc,Zr) alloys at ambient and elevated temperatures. Acta Mater 51(16):4803–4814
22. Robson JD (2004) A new model for prediction of dispersoid precipitation in aluminium alloys containing zirconium and scandium. Acta Mater 52:1409–1421
23. Belov NA, Alabin AN, Eskin DG, Istomin-Kastrovskii VV (2006) Optimization of hardening of Al-Zr-Sc cast alloys. j Mater Sci 41:5890–5899
24. Knipling KE, Karnesky RA, Lee CP, Seidman DN (2010) Precipitation evolution in Al-0.1Sc, Al-0.1Zr and Al-0.1Sc-0.1Zr (at.%) alloys during isochronal aging. Acta Mater 58(15):5184–5195

25. Rokhlin LL, Bochvar NR, Leonova NP (2011) Study of decomposition of oversaturated solid solution in Al-Sc-Zr alloys at different ratio of scandium and zirconium. Inorg Materials: Appl Res 2:517–520
26. Knipling KE, Dunand DC (2008) Creep resistance of cast and aged Al-0.1Zr and Al-0.1Zr-0.1Ti (at.%) alloys at 300–400 °C. Scr Mater 59(4):387–390
27. Wen SP, Gao KY, Li Y, Huang H, Nie ZR (2011) Synergetic effect of Er and Zr on the precipitation hardening of Al-Er-Zr alloy. Scr Mater 65(7):592–595
28. Li H, Bin J, Liu J, Gao Z, Lu X (2012) Precipitation evolution and coarsening resistance at 400 °C of Al microalloyed with Zr and Er. Scr Mater 67(1):73–76
29. Wen SP, Gao KY, Huang H, Wang W, Nie ZR (2013) Precipitation evolution in Al-Er-Zr alloys during aging at elevated temperature. J All Comp 574:92–97
30. Li H, Gao Z, Yin H, Jiang H, Su X, Bin J (2013) Effects of Er and Zr additions on precipitation and recrystallization of pure aluminum. Scr Mater 68(1):59–62
31. Gao H, Feng W, Wang Y, Gu J, Zhang Y, Wang J, Sun B (2016) Structural and compositional evolution of Al3(Zr,Y) precipitates in Al-Zr-Y alloy. Mater Charact 121:195–198
32. Huang H, Wen SP, Gao KY, Wan W, Nie ZR (2013) Age hardening behavior and corresponding microstructure of dilute Al-Er-Zr alloys. Metall Mater Trans A 44:2849–2856
33. Gao Z, Li H, Lai Y, Ou Y, Li D (2013) Effects of minor Zr and Er on microstructure and mechanical properties of pure aluminum. Mater Sci Eng A 580:92–98
34. Mikhaylovskaya AV, Kotov AD, Pozdniakov AV, Portnoy VK (2014) A high-strength aluminium-based alloy with advanced superplasticity. J All Comp 599:139–144
35. Kotov AD, Mikhaylovskaya AV, Borisov AA, Yakovtseva OA, Portnoy VA (2017) High-strain-rate superplasticity of the Al-Zn-Mg-Cu alloys with Fe and Ni additions. Phys Met Met 118:913–921
36. Kotov AD, Mikhaylovskaya AV, Portnoy VK (2014) Effect of the solid-solution composition on the superplasticity characteristics of Al-Zn-Mg-Cu-Ni-Zr alloys. Phys Met Met 115:730–735
37. Petrova AN, Brodova IG, Razorenov SV, Shorokhov EV, Akopyan TK (2019) Mechanical properties of the Al-Zn-Mg-Fe-Ni alloy of eutectic type at different strain Rates. Phys Met Met 120:1221–1227
38. Brodova IG, Shirinkina IG, Yu. Rasposienko D, Akopyan TK (2020) Structural evolution in the quenched Al-Zn-Mg-Fe-Ni Alloy during severe plastic deformation and annealing. Phys Met Met 121:899–905
39. Shirinkina IG, Brodova IG (2020) Annealing-induced structural-phase transformations in an Al-Zn-Mg-Fe-Ni alloy after high pressure torsion. Phys Met Met 121:344–351
40. Pozdniakov AV, Barkov RY (2018) Microstructure and materials characterisation of the novel Al-Cu-Y alloy. Mater Sci Tech 34(12):1489–1496
41. Amer SM, Barkov RY, Yakovtseva OA, Pozdniakov AV (2020) Comparative analysis of structure and properties of quasibinary Al-6.5Cu-2.3Y and Al-6Cu-4.05Er alloys. Phys Met Met 121(5):476–482
42. Pozdnyakov AV, Barkov RYu , Sarsenbaev Z, Amer SM, Prosviryakov AS (2019) Evolution of microstructure and mechanical properties of a new Al-Cu-Er wrought alloy. Phys Met Met 120(6):614–619
43. Pozdniakov AV, Barkov RY, Amer SM, Levchenko VS, Kotov AD, Mikhaylovskaya AV (2019) Microstructure, mechanical properties and superplasticity of the Al-Cu-Y-Zr alloy. Mater Sci Eng A 758:28–35
44. Amer SM, Barkov RYu , Yakovtseva OA, Loginova IS, Pozdniakov AV (2020) Effect of Zr on microstructure and mechanical properties of the Al-Cu-Er alloy. Mater Sci Tech 36(4):453–459
45. Amer SM, Mikhaylovskaya AV, Barkov RYu , Kotov AD, Mochugovskiy AG, Yakovtseva OA, Glavatskikh MV, Loginova IS, Medvedeva SV, Pozdniakov AV (2021) Effect of homogenization treatment regime on microstructure, recrystallization behavior, mechanical properties, and superplasticity of Al-Cu-Er-Zr alloy. JOM 73(10):3092–3101
46. Amer SM, Barkov RYu , Pozdniakov AV (2020) Effect of Mn on the phase composition and properties of Al-Cu-Y-Zr alloy. Phys Met Met 121(12):1227–1232
47. Amer S, Yakovtseva O, Loginova I, Medvedeva S, Al. Prosviryakov, Bazlov A, Barkov R, Pozdniakov A (2020) The phase composition and mechanical properties of the novel precipitation-strengthening Al-Cu-Er-Mn-Zr alloy. Appl Sci 10:5345
48. Amer SM, Barkov RY, Prosviryakov AS, Pozdniakov AV (2021) Structure and properties of new heat-resistant cast alloys based on the Al-Cu-Y and Al-Cu-Er systems. Phys Met Met 122:908–914
49. Amer SM, Barkov RY, Prosviryakov AS, Pozdniakov AV (2021) Structure and properties of new wrought Al-Cu-Y and Al-Cu-Er based alloys. Phys Met Met 122:915–922
50. Glavatskikh MV, Barkov RYu , Khomutov MG, Pozdniakov AV (2022) The effects of yttrium and erbium on the phase composition and aging of the Al-Zn-Mg-Cu-Zr Alloy with a high copper content. Phys Met Met 123:617–623
51. Zolotarevskii VS, Belov NA (2005) Material science of cast aluminum alloys. MISiS, Moscow (in Russian)
52. Kaufman JG (1999) Properties of aluminum alloys: tensile, creep, and fatigue data at high and low temperatures. ASM Intern.

Authors and Affiliations

✉ M. V. Glavatskikh
glavatskikh@edu.misis.ru

R. Yu. Barkov
barkov@misis.ru

M. G. Khomutov
khomutov@misis.ru

A. V. Pozdniakov
pozdniakov@misis.ru

M. V. Glavatskikh, R. Yu. Barkov, M. G. Khomutov, A. V. Pozdniakov
National University of Science and Technology MISIS, Moscow, Russian Federation